Research Article Open Access

tance [5, 6].

alloys.

ement Gd.

Miao Yang*, Zhiyi Zhang, Yaohui Liu, and Xianlong Han

Corrosion and mechanical properties of AM50 magnesium alloy after modified by different amounts of rare earth element Gadolinium

DOI 10.1515/phys-2016-0049 Received May 30, 2016; accepted Sep 20, 2016

Abstract: To improve the corrosion and mechanical properties of the AM50 magnesium alloy, different amounts of the rare earth element gadolinium were used. The microstructure, corrosion and mechanical properties were evaluated by X-ray diffraction, scanning electron microscopy, energy dispersive spectroscopy, and electrochemical and mechanical stretch methods. The results indicate that, with Gd addition, the amount of the Al₂Gd₃ phase increased while the β -Mg₁₇Al₁₂ phase amount decreased. Due to the Gd addition, the grain of the AM50 magnesium alloy was significantly refined, which improved its tensile strength. Further, the decrease in the amount of the β phase improved the corrosion resistance of the alloy. The fracture mechanism of the Gd-modified AM50 magnesium alloy was a quasi-cleavage fracture. Finally, the optimum corrosion residual strength of the AM50 magnesium alloy occurred with 1 wt.% of added Gd.

Keywords: magnesium alloy; rare earth; corrosion; corrosion residual strength

PACS: 81.40Np

1 Introduction

Magnesium alloys are the lightest structure metal, and have therefore been called "the 21st Century Green Structure Metal" [1]. Magnesium alloys are promising candidates to replace steel and aluminum alloys in many strucRare earth elements, sometimes called "metal vitamins" because of their unique attribute of improving the performance of metals, have been used to modify magnesium alloys for several years. For instance, Wang [8], Li [9] and Song [10] have studied the effects of the rare earth elements Y, Ce and Nd upon the corrosion resistance of magnesium alloys. Gadolinium is a prime candidate as a modifying rare earth element for magnesium alloy. The extranuclear electron arrangement of Gd is $4f^75d^16s^2$, where the 4f electron orbit is a half-filled state that creates a stable electron structure. The atomic radius of Gd is large, and the two outer-layer s electrons and the single second-outer-layer 5d electron are easy to lose. Further, Gd can become a positive trivalent ion with high chemical activ-

ity, which produces a strong binding force with atoms such as O and S. To date, the corrosion and mechanical properties of Gd-modified AM50 magnesium alloys have been investigated infrequently. This paper, therefore, investigates

modifying the corrosion and mechanical properties of a

cast AM50 magnesium alloy by adding the rare earth el-

tural and mechanical applications owing to their attractive

properties of excellent castability, good machinability, superior damping capacity, outstanding stiffness-to-weight

ratio, and ease of recyclability [2-4]. The AM50 alloy is one

of the most successfully-used magnesium alloys in the au-

tomotive industry; however, its application is still limited

by its strength and most especially its poor corrosion resis-

loss of the mechanical properties that accompanies the

corrosion process is thus also inevitable. Here, the tensile

strength of the materials tested after a corrosion test was

defined as the corrosion residual strength (CRS), and the

study of the CRS of materials is of great significance to pre-

dict their service life [7]. Therefore, building an evaluation

system for CRS will promote the application of magnesium

Typically, corrosion is inevitable with usage, and the

Zhiyi Zhang, Xianlong Han: Engineering Training Center; Beihua University, Jilin 132021, China

Yaohui Liu: College of Materials Science and Engineering; Jilin University, Changchun 130025, China

© 2016 M. Yang *et al.*, published by De Gruyter Open.

This work is licensed under the Creative Commons Attribution-NonCommercial-NoDerivs 3.0 License.

^{*}Corresponding Author: Miao Yang: Engineering Training Center; Beihua University, Jilin 132021, China; College of Materials Science and Engineering; Jilin University, Changchun 130025, China; Email: vangmiao1021@163.com

2 Experimental

2.1 Preparation of sample

The experimental alloys used in this study were a commercial AM50 Mg alloy, a Mg-Gd master alloy (Gd = 20 wt.%) and industry-pure Al. The casting equipment were a well-type electric resistance furnace and a graphite crucible. First, the AM50 Mg alloy was re-melted in a highly-pure argon environment. When the temperature of the furnace was ~720°C, the Mg-Gd master alloy and pure Al were placed into the melting AM50 Mg alloy liquid. The melting alloy was stirred and standed for 20 min. Then the melting alloy was cast into the mold at the temperature of 710° C. where the size of the cast ingot was $200 \times 130 \times 12 \text{ mm}^3$. The samples were denoted as AM50GdX (where X represents the content of Gd), and their compositions are listed in Table 1.

2.2 Tensile test

The specimens used for tensile testing were cut to $120\times12\times12 \text{ mm}^3$ and lathed into their final shape, with the dimensions shown in Fig. 1. The samples were first polished, and then washed and dried. Tensile tests equipment was an AG-10TA materials tensile test machine. The stretching rate was 1 mm min⁻¹. The lowest strength obtained from three identical samples measured under the same corrosion time was recorded as the safety corrosion

Table 1: Compositions of the Gd-modified AM50 Mg alloys

Sample named	Gd (wt.%)	AM50 (wt.%)
AM50Gd1	0.5	Bal.
AM50Gd2	1.0	Bal.
AM50Gd3	1.5	Bal.
AM50Gd4	2.0	Bal.

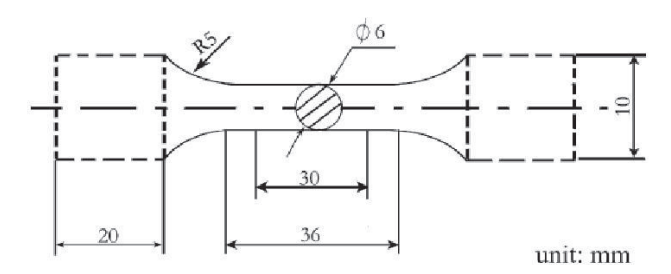


Figure 1: Diagrammatic sketch of the tensile test sample with its dimension.

residual strength if the samples were without any pores or slag.

2.3 Corrosion process

The corrosion immersion tests were carried out in a 3.5 wt.% NaCl solution made with analytical reagent chemicals and distilled water. Before testing, an Mg(OH)₂ powder was placed in the test solution to obtain a saturated Mg(OH)₂ NaCl solution, which could produce a consistent rate of corrosion [7]. The immersion test was performed at 25°C in a constant-temperature chamber for a corrosion time of 24, 72, 168, 264, 336 and 432 h, separately [7]. At each time point, three tensile test samples were removed from the corrosion solution and washed with a chromic-acid silver-nitrate aqueous solution and with absolute ethyl alcohol, and were subsequently dried with cold flowing air. Finally, the tensile test samples were stored in numbered sample bags.

2.4 Metallographic sample process

The samples used for microstructural observation were corroded using 3.5 wt.% nitric acid ethyl alcohol for 30 s. The microstructure, the main view and vertical sections of the corroded samples were recorded and analyzed by a scanning electron microscope (SEM; JSM-5600, JEOL Inc.). A detailed analysis of the phases present within each sample was carried out via X-ray diffractometry (XRD; LabX XRD-6000, Shimadzu).

2.5 Electrochemical polarization test

Electrochemical polarization tests were carried out in a LK98B11 chemical workstation (Lanlike), with an exposed area of $10\times10~\text{mm}^2$ and where the test solution was a 3.5 wt.% NaCl aqueous solution. A standard three-electrode configuration was used, wherein saturated calomel was used as a reference electrode, platinum as a standard electrode and the sample as the working electrode. Specimens were immersed in the test solution and a polarization scan was carried out at a rate of $10~\text{mV s}^{-1}$.

446 — M. Yang et al. DE GRUYTER OPEN

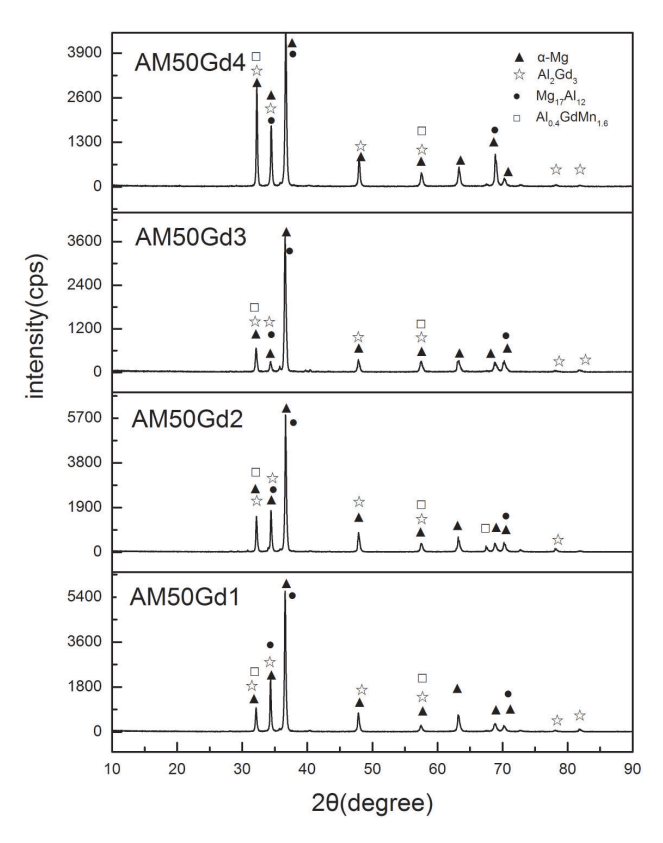


Figure 2: X-ray diffraction spectra from the Gd-modified AM50 magnesium alloys. The samples are AM50 Mg alloy modified with Gd in the amount of 0.5 wt.% (AM50Gd1), 1.0 wt.% (AM50Gd2), 1.5 wt.% (AM50Gd3) and 2.0 wt.% (AM50Gd4).

3 Results and discussion

3.1 Microstructure

The XRD spectra of the Gd-modified AM50 magnesium alloy samples are shown in Fig. 2, where the phases existing in the alloy include $\alpha\text{-Mg}$, $\beta\text{-Mg}_{17}\text{Al}_{12}$, $\text{Al}_{0.4}\text{GdMn}_{1.6}$ and Al_2Gd_3 . From the Mg-Al phase diagram, the Mg and Al (4.427 wt.%) in the AM50 magnesium alloy during the solidification process are present in the $\alpha\text{-Mg}$ and $\beta\text{-Mg}_{17}\text{Al}_{12}$ phases. After Gd was added, the Al, Gd and Mn form Al_2Gd_3 and $\text{Al}_{0.4}\text{GdMn}_{1.6}$, where the diffraction peak intensity of the Al_2Gd_3 and $\text{Al}_{0.4}\text{GdMn}_{1.6}$ phases increases with the addition of Gd while that of the $\beta\text{-Mg}_{17}\text{Al}_{12}$ phase decreases.

The microstructure morphology of the as-cast AM50 magnesium alloy and the AM50GdX alloys (where X represents the content of Gd) are illustrated using SEM images in Fig. 3. The original microstructure of the as-cast AM50 magnesium alloy comprises primarily the α -Mg phase (medium intensity areas in the SEM image) and the high-intensity island-shaped β -Mg₁₇Al₁₂ phase (Fig. 3(a)). Af-

ter Gd is added, the brighter-intensity small-grain Al₂Gd₃ and Al_{0.4}GdMn_{1.6} exist at the grain boundaries (Figs. 3(b)– 3(e)). With increasing amounts of Gd, the amount of brighter-intensity small-grain Al₂Gd₃ and Al_{0.4}GdMn_{1.6} phases increases, while the amount and volume of the β -Mg₁₇Al₁₂ phase decreases. From Fig. 3(b) it can be seen that, when the Gd content is 0.5 wt.%, the amount of β phase noticeably decreases and the visible Al₂Gd₃ and Al_{0.4}GdMn_{1.6} phases are few. When 1 wt.% Gd is added, the amount of the phases containing Gd increases and the amount of the β phase noticeably decreases (Fig. 3(c)). When 1.5 wt.% Gd is added (Fig. 3(d)), the amount and volume of high-intensity Al₂Gd₃ and Al_{0.4}GdMn_{1.6} phases increases further. Finally, with 2.0 wt.% of added Gd (Fig. 3(e)), the β -phase areas become as small as the areas containing the Al₂Gd₃ and Al_{0.4}GdMn_{1.6} phases.

The SEM morphology of AM50Gd2 and the energy dispersive spectroscopy (EDS) results from two points (labeled A and B) are shown in Fig. 4c. Under 5000× magnification, many smaller areas of the β phase are observed, and the Al_{0.4}GdMn_{1.6} and Al₂Gd₃ phases are seen to accompany one another. During the solidification process, Gd exhibits a preference for combining with Al over Mg [11]. Owing to its higher melting point than that of the α -Mg and β -Mg₁₇Al₁₂ phases, the high-strength and thermally stable Al₂Gd₃ phase separates out first at the front of the solidification interface. This inhibits the separation of the β -Mg₁₇Al₁₂ phase and refines the microstructure of the alloy. The rare earth element Gd, therefore, improves the nucleation rate and leads to grain refinement and grain boundary strengthening of the AM50 magnesium alloy.

3.2 Mechanical character

Figure 5 shows the engineering stress-strain curves of the AM50GdX magnesium alloys. The tensile strength of the AM50 magnesium alloy after Gd modification is found to increase with Gd addition, with the values 210 MPa (Gd = 0.5 wt.%), 214 MPa (Gd = 1.0 wt.%), 215 MPa (Gd = 1.5 wt.%) and 220 MPa (Gd = 2.0 wt.%). It can be observed that the curves from the varying alloys are similar in shape and consist of the two ranges of linear elastic and plastic zones, where the plastic zone is markedly longer than the linear zone. With the increase of Gd content, the slopes of the curves initially increase and then decrease. The incorporation of rare earth element Gd causes grain refinement strengthening and grain boundary strengthening, which improves the tensile properties of the AM50 magnesium alloy. However, excessive quantities of Gd lead to a reduction in the slope of the engineering stress-strain curve,

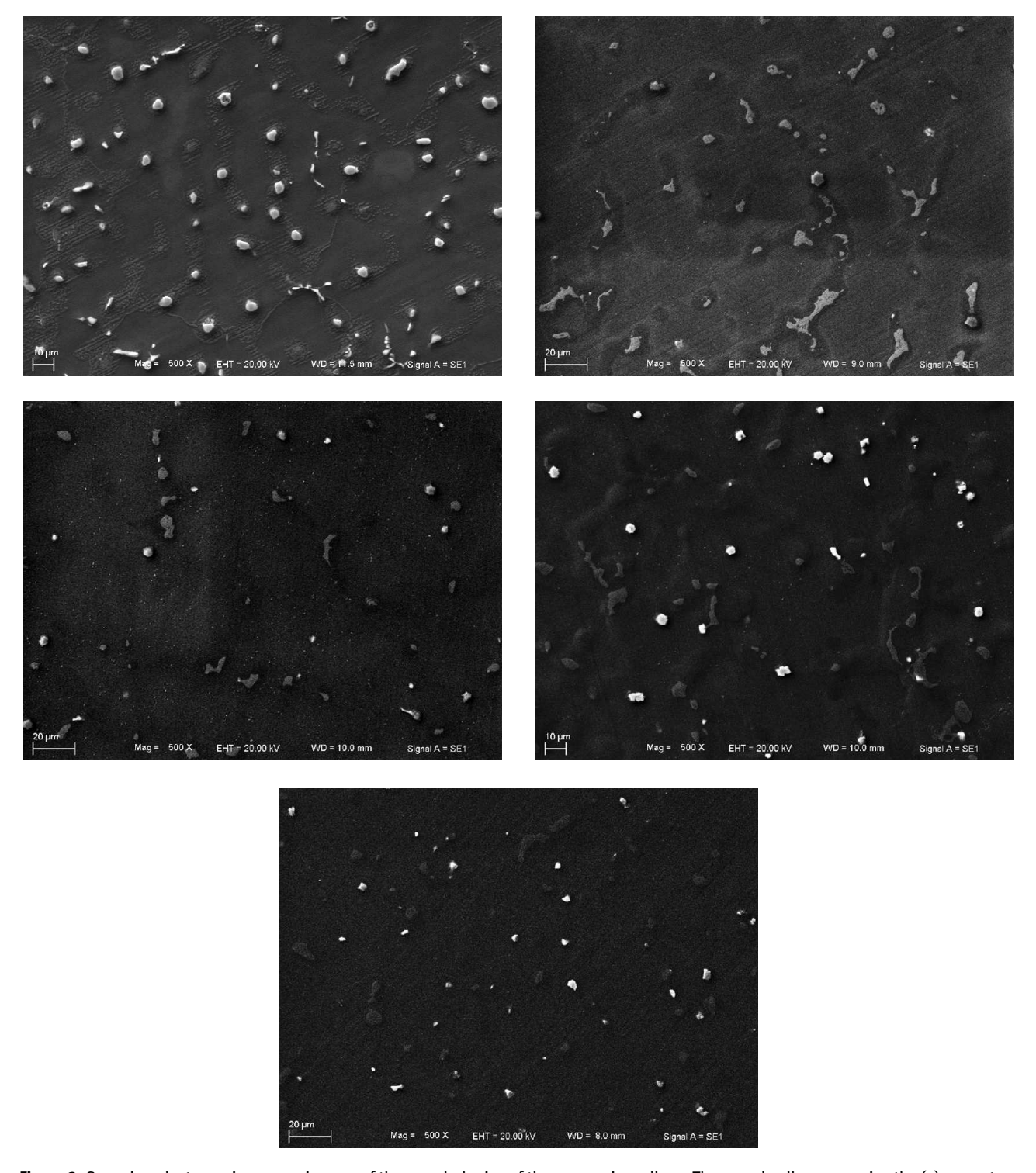
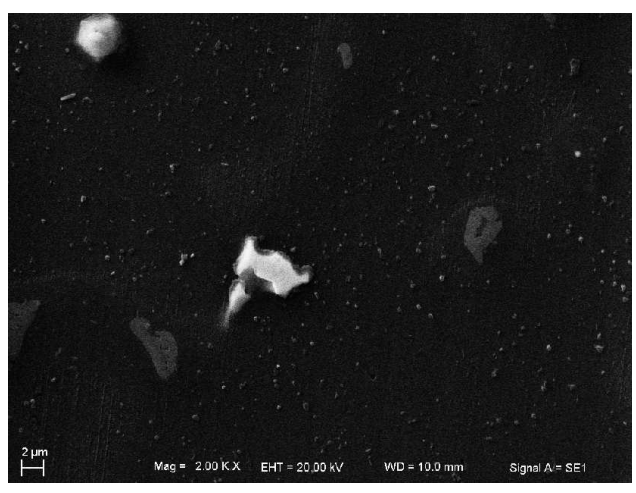


Figure 3: Scanning electron microscope images of the morphologies of the magnesium alloys. The sample alloys comprise the (a) as-cast AM50, (b) AM50Gd1 containing 0.5 wt.% Gd, (c) AM50Gd2 containing 1.0 wt.% Gd, (d) AM50Gd3 containing 1.5 wt.% Gd, and (e) AM50Gd4 containing 2.0 wt.% Gd.

which means that the elongation of the alloy is improved via the plastic deformation properties and that the toughness is reduced at the same time. Further, the shape of the stress-strain curves reveals that the fracture mode of the AM50GdX magnesium alloy is quasi-cleavage fracture.

448 — M. Yang et al. DE GRUYTER OPEN



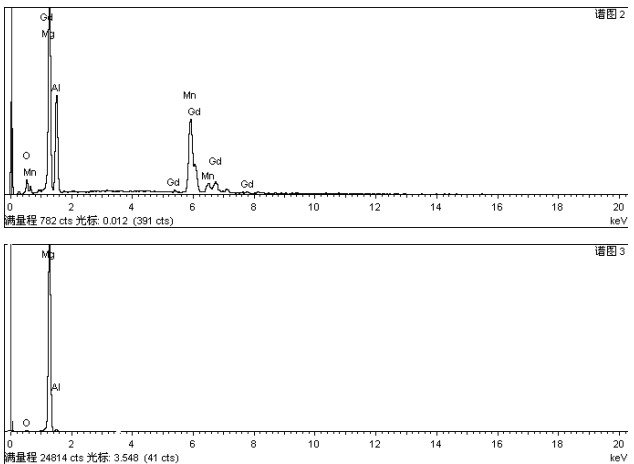


Figure 4: Scanning electron microscope images of the morphology and energy dispersive X-ray spectra of the AM50Gd2 sample containing 1.0 wt.% added Gd. The image (left) shows the points from where the spectra for point A (upper right) and point B (lower right) are obtained.

3.3 Corrosion character

Figure 6 shows Tafel curves of AM50GdX magnesium alloy, where the corrosion potentials of the AM50Gd1–AM50Gd4 magnesium alloys are –1.65, –1.75, –1.72 and –1.71 V, respectively. In this range, with an increasing amount of Gd, the corrosion potential initially decreases and then increases. Simultaneously, the corrosion current density of the cathodic branch initially decreases and then increases. The turning point for both of these parameters is 1.0 wt.% Gd (AM50Gd2). Owing to the significant difference between the Gd and Mg atoms, it is difficult to solid-solute the Gd atom into the AM50 magnesium alloy, but instead the Gd tends to form rare earth compounds. When the Gd amount is less than 1.0 wt.%, the effect of Gd addition is grain refinement, which reduces the micro-galvanic effect [7, 12]. However, with more Gd the amount and vol-

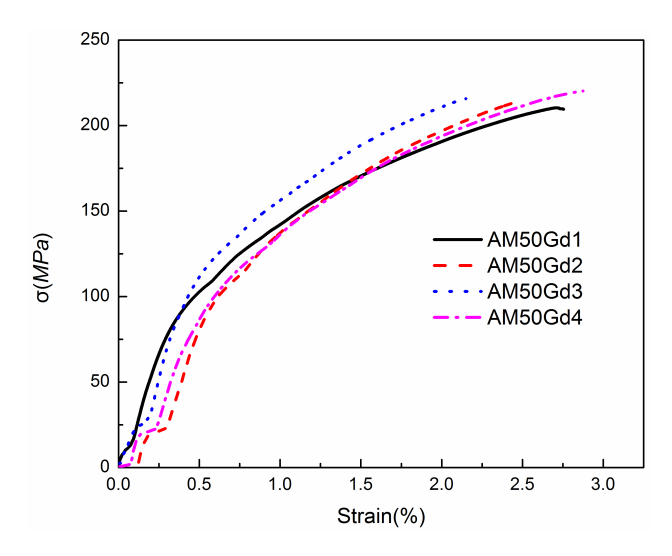


Figure 5: The engineering stress-strain curves of AM50GdX magnesium alloys. The samples are AM50 Mg alloy modified with Gd in the amount of 0.5 wt.% (AM50Gd1), 1.0 wt.%

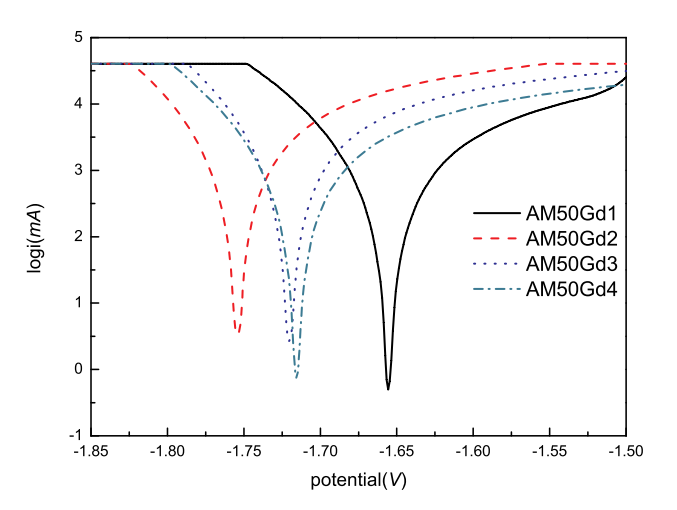


Figure 6: Tafel curves of the AM50GdX magnesium alloys. The samples are AM50 Mg alloy modified with Gd at 0.5 wt.% (AM50Gd1), 1.0 wt.%

ume of the Al_2Gd_3 phase significantly increases, which leads to an aggravation of the micro-galvanic effect and a hydrogen evolution reaction. This explains why corrosion resistance worsens after adding more than 1 wt.% Gd.

The surface corrosion morphologies of the AM50GdX samples after a 24 h immersion in the corrosion solution are shown in Fig. 7. Corrosion pitting appears on all of the sample surfaces after 24 h immersion in NaCl aqueous solution, but the amount of corrosion pitting still follows the trend of initially decreasing and then increasing as the Gd amount increases. Interestingly, the turning point for the maximum pitting also appears at AM50Gd2 (Gd = 1 wt.%). During the corrosion process in aqueous solution, the oxide or hydroxide film on the surface of the magnesium al-

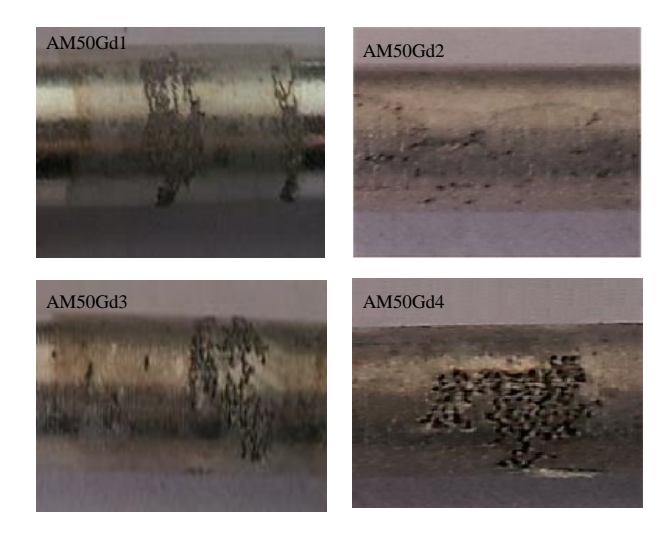


Figure 7: The surface corrosion morphology of the AM50GdX samples after 24 h immersion in the corrosion solution. The samples shown are AM50 Mg alloy modified with Gd at 0.5 wt.% (AM50Gd1, upper left), 1.0 wt.% (AM50Gd2, upper right), 1.5 wt.% (AM50Gd3, lower left) and 2.0 wt.% (AM50Gd4, lower right).

loy protects the magnesium alloy matrix, and so the quality of the oxide or hydroxide film determines the corrosion pitting nucleation rate. The rare earth element Gd contributes to the formation of a high-quality oxide or hydroxide film, but when the Gd addition is over 1.0 wt.% the quality of the oxide or hydroxide film worsens. The addition of excessive amounts of Gd leads to an increase of the Al-Gd phase, which destroys the oxide or hydroxide film, and the corrosion pitting and corrosion current begins to increase. Because the atoms of the rare earth element tend to be attracted to each other [13], they form atomic clusters that lead to the Al-Gd phase segregation. Figure 7 (bottom right labeled AM50Gd4) gives evidence of the corrosion pitting concentrated on a localized region of this sample containing Gd = 2.0 wt.%.

3.4 Corrosion residual strength(CRS)

Figure 8 shows the corrosion residual strength (CRS) curves of the AM50GdX magnesium alloys where it can be seen that, for a corrosion time greater than 168 h, the CRS value of the AM50GdX samples decreases linearly. Further, at each time point above 168 h the CRS value of the AM50Gd2 sample is greater than that of the others, signifying that 1 wt.% Gd addition is beneficial for improving the CRS of AM50 magnesium. In the CRS curve of AM50Gd1 (Gd = 0.5 wt.%), the reduction rate of the CRS value showed that there are two interregional: the beginning of the corrosion process for this sample the corrosion rate is higher,

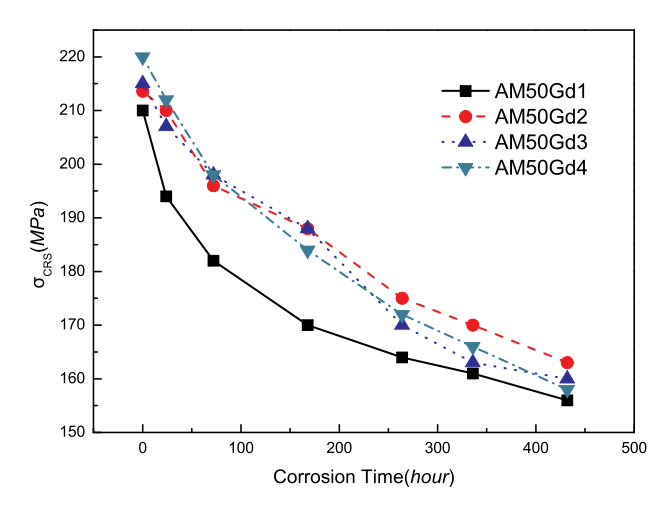


Figure 8: The corrosion residual strength (σ_{CRS}) vs. corrosion time for the AM50GdX magnesium alloys. The samples are AM50 Mg alloy modified with Gd at 0.5 wt.% (AM50Gd1), 1.0 wt.% (AM50Gd2), 1.5 wt.% (AM50Gd3) and 2.0 wt.% (AM50Gd4).

but after about 150 h into the corrosion process the corrosion rate reduces. This is because, after 150 h of immersion in the NaCl aqueous solution, the oxide or hydroxide film formed on the surface of the AM50Gd1 sample is in a stable state, and the type of corrosion is therefore a uniform corrosion [14]. The CRS curves of the AM50Gd2, AM50Gd3 and AM50Gd4 samples exhibit a different trend, however, wherein the CRS value reduces in a linear fashion throughout the corrosion process. Therefore, the depth of the corrosion pitting on the AM50Gd2, AM50Gd3 and AM50Gd4 samples increases until the steady stage.

In previous study [7], it is found that the existence and development of corrosion pits are the direct reason for the dropping of the tensile strength. First, corrosion pits present leads to a decrease of the CRS value directly because of the decrease of the cross-sectional area. Second, the stress concentration at the large change of curvature in the corrosion pits and the emergence of micro-cracks at the bottom of the corrosion pits causes fracture of the tensile samples. Through statistics and calculations, the stress concentration is more important than the depth of the corrosion pits. Therefore, reducing the corrosion pits is beneficial for improving the CRS of these AM50GdX samples.

With the tensile test samples immersed in the corrosion solution, the external and internal corrosion factors of the magnesium alloy interact at the surface of the samples [15], which leads to the nucleation and growth of the corrosion pitting. The presence of Gd contributes in two ways to affect the CRS value of the AM50 magnesium alloy, via the strengthening of its tensile properties and the improvement of its corrosion resistance. First, the methods

whereby the AM50 magnesium alloy is strengthened by Gd addition are owing to grain refinement, grain boundary and second-phase strengthening. Second, Gd improves the corrosion resistance. In the corrosion process, corrosion pitting nucleates at the α -Mg phase because the corrosion potential of the β phase and the Al-Gd phase are higher than that of α -Mg phase [7]. Therefore, after Gd addition the nucleation of corrosion pitting becomes more difficult.

4 Conclusions

The corrosion and mechanical performance of a Gdmodified AM50 magnesium alloy have been studied. It was found that the phases within the Gd-modified AM50 magnesium alloy include the α -Mg, β -Mg₁₇Al₁₂, Al₂Gd₃ and Al_{0.4}GdMn_{1.6} phases. The rare earth element Gd contributes toward grain refinement, grain boundary strengthening and second-phase strengthening to improve the tensile strength of the alloy. Further, Gd also improves the corrosion resistance of the AM50 magnesium alloy by reducing the β -Mg₁₇Al₁₂ phase. However, with increasing amounts of added Gd, the corrosion resistance of AM50 initially improves and then worsens, where the turning point for this corrosion resistance is at 1.0 wt.% Gd addition. It is therefore concluded that the corrosion residual strength of the 1.0 wt.% Gd-modified AM50 magnesium alloy (AM50Gd2) is higher than that of the other AM50GdX alloys tested.

Acknowledgement: This study was supported by the Science and Technology Development Projects of Changchun City (No.11KZ31), the National Natural Science Foundation of China(No.51201068), Science and Technology Development Projects of Jilin Province (No. 201201032) and the Fundamental Research Funds for the Central Universities (Jilin University, Grant No. 2013ZY04)

References

- [1] Yang M., Liu Y.H., Jin H.Z., Song Y.L., Influence of solid-solution treatment on tensile properties of cast AM50 magnesium alloy after corrosion tests, J. Tran. Mater. heat treat., 2012, DOI:10.13289/j.issn.1009-6264.2012.07.020
- [2] Zeng R.C., Chen J., Dietzle W., Zettler R. Santos J.F., Nascimento M.L., et al., Corrosion of friction stir welded magnesium alloy AM50, J.Cor. Sci., 2009, http://www.sciencedirect.com/scie nce/article/pii/S0010938X09001875

- [3] Shi Z.M., Song G.L., Atrens A., Influence of anodising current on the corrosion resistance of anodised AZ91D magnesium alloy, J. Cor. sci., 2006, http://www.sciencedirect.com/science/artic le/pii/S0010938X0500243X
- [4] Wu G.H., Fan Y., Gao H.T., Zhai C.Q., Zhu Y.P., The effect of Ca and rare earth elements on the microstructure, mechanical properties and corrosion behavior of AZ91D, J. Mater. Sci. Eng. A, 2005, http://www.sciencedirect.com/science/article/pii/S09215093 05009342
- [5] Zhou W., Shen T., Aung N.N., Effect of heat treatment on corrosion behaviour of magnesium alloy AZ91D in simulated body fluid, J. Cor. Sci., 2010, http://www.sciencedirect.com/science/article/pii/S0010938X09005848
- [6] Pardo A., Merino M.C., Coy A.E., Arrabal R., Viejo F., Matykina E., Corrosion behaviour of magnesium/aluminium alloys in 3.5 wt.% NaCl, J. Cor. Sci., 2008, http://www.sciencedirect.com/science/article/pii/S0010938X07003125
- [7] Yang M., Liu Y.H., Liu J.A., Song Y.L., Effect of T6 heat treatment on corrosion resistance and mechanical properties of AM50 magnesium alloy, Mater. Res. Innovat., 2015, http://www.tandfonline.com/doi/abs/10.1179/1432891715Z.000000 0002160
- [8] Wang Q., Liu Y.H., Zhu X.Y., Li S., Yu S.R., Zhang L.N., et al., Study on the effect of corrosion on the tensile properties of the 1.0 wt.% Yttrium modified AZ91 magnesium alloy, J. Mat. Sci. Eng. A, 2009, http://www.sciencedirect.com/science/article/pii/S092150930900402X
- [9] Li C.F., Liu Y.H., Wang Q., Zhang L.N., Zhang D.W., Study on the corrosion residual strength of the 1.0 wt.% Ce modified AZ91 magnesium alloy, J. Mater. Char., 2009, http:// www.sciencedirect.com/science/article/pii/S1044580309002 927
- [10] Song, Y.L., Liu, Y.H., Yu, S.R., Zhu X.Y., Wang S.H., Effect of neodymium on microstructure and corrosion resistance of AZ91 magnesium alloy, J. Mater. Sci., 2007, doi:10.1007/s10853-006-0661-z
- [11] Wang L., Zhang B.P., Shinohara T., Corrosion behavior of AZ91 magnesium alloy in dilute NaCl solutions, Mater. Des., 2010, http://www.sciencedirect.com/science/article/pii/S02613069 09003902
- [12] Song G.L., Bowles A.L., StJohn D.H., Corrosion resistance of aged die cast magnesium alloy AZ91D, J. Mat. Sci. Eng. A, 2004, http://www.sciencedirect.com/science/article/pii/S09215093 03008177
- [13] Liu G.L., Electronic theoretical study on the influence of rare earth on the stress corrosion in magnesium alloy, J. Acta Phy. sin., 2006, http://www.cnki.net/KCMS/detail/det ail.aspx?QueryID=15&CurRec=7&recid=&filename=WLXB2006 12063&dbname=CJFD2006&dbcode=CJFQ&pr=&urlid=&yx=& uid=WEEvREcwSlJHSldRa1Fhb09jeVVYampBSGJZQjY5VVBiTkdR RXRFL1M2QT0=\$9A4hF_YAuvQ5obgVAqNKPCYcEjKensW4gg18F m4gTkoUKalD8j8gFw!!&v=MDc2MTZWNy9LTWIIVGJMRzRIdGZO clk5RFo0UjhlWDFMdXhZUzdEaDFUM3FUcldNMUZyQ1VSTHllWit kdEZ5M20=
- [14] Song D., Ma A.B., Jiang J.H., Lin P.H., Yang D.H., Fan J.F., Corrosion behavior of equal-channel-angular-pressed pure magnesium in NaCl aqueous solution, J. Cor. Sci. 2010, http://www.sciencedirect.com/science/article/pii/S0010938X09004879
- [15] Liu W.J., Cao F.H., Chang L.R., Zhang Z., Zhang J.Q., Effect of rare earth element Ce and La on corrosion behavior of AM60

magnesium alloy, J. Cor. Sci., 2009, http://www.sciencedir ect.com/science/article/pii/S0010938X09001103